7-28-2023

First High-Speed Video Camera Observations of a Lightning Flash Associated With a Downward Terrestrial Gamma-Ray Flash

R. U. Abbasi
Loyola University of Chicago

M. M.F. Saba
Instituto Nacional de Pesquisas Espaciais

J. W. Belz
The University of Utah

P. R. Krehbiel
New Mexico Institute of Mining and Technology

W. Rison
New Mexico Institute of Mining and Technology

See next page for additional authors

Follow this and additional works at: https://ecommons.luc.edu/physics_facpubs

Recommended Citation

Authors

R. U. Abbasi, M. M.F. Saba, J. W. Belz, P. R. Krehbiel, W. Rison, N. Kieu, D. R. da Silva, M. A. Stanley, Dan Rodeheffer, J. Remington, J. Mazich, R. LeVon, K. Smout, A. Petrizze, T. Abu-Zayyad, M. Allen, R. Arimura, E. Barcikowski, D. R. Bergman, S. A. Blake, I. Buckland, B. G. Cheon, M. Chikawa, T. Fujii, K. Fujisue, K. Fujita, and R. Fujiwara

AGU ADVANCING EARTH AND SPACE SCIENCES

Geophysical Research Letters®

Key Points:
- Simultaneous recordings of a downward-directed terrestrial gamma-ray flash (TGF), high-speed video images, and radio emissions
- TGF events occurred while the leader was already branching below cloud base and even when it was halfway in its propagation to ground
- Energetic downward-directed TGFs were associated with fast downward leaders that produced high return stroke peak currents
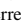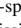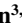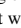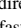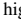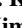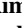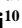
First High-Speed Video Camera Observations of a Lightning Flash Associated With a Downward Terrestrial Gamma-Ray Flash

R. U. Abbasi[1], M. M. F. Saba[2], J. W. Belz[3], P. R. Krehbiel[4], W. Rison[4], N. Kieu[1], D. R. da Silva[2], M. A. Stanley[4], Dan Rodeheffer[4], J. Remington[3,5], J. Mazich[1], R. LeVon[6], K. Smout[6], A. Petrizze[6], T. Abu-Zayyad[1,6], M. Allen[6], R. Arimura[6], E. Barcikowski[3], D. R. Bergman[3], S. A. Blake[3], I. Buckland[3], B. G. Cheon[7], M. Chikawa[8], T. Fujii[6,9], K. Fujisue[8], K. Fujita[8], R. Fujiwara[6], M. Fukushima[8], G. Furlich[3], N. Globus[10,11], R. Gonzalez[3], W. Hanlon[3], N. Hayashida[12], H. He[10], K. Hibino[12], R. Higuchi[10], K. Honda[13], D. Ikeda[12], N. Inoue[14], T. Ishii[13], H. Ito[10], D. Ivanov[3], H. Iwakura[15], A. Iwasaki[6], H. M. Jeong[16], S. Jeong[16], C. C. H. Jui[3], K. Kadota[17], F. Kakimoto[12], O. Kalashev[18], K. Kasahara[19], S. Kasami[20], S. Kawakami[6], K. Kawata[8], I. Kharuk[18], E. Kido[10], H. B. Kim[7], J. H. Kim[3,21], J. H. Kim[3], S. W. Kim[16], Y. Kimura[6], I. Komae[6], Y. Kubota[15], M. Kuznetsov[18,22], Y. J. Kwon[23], K. H. Lee[16], B. Lubsandorzhiev[18], J. P. Lundquist[3,24], T. Matsuyama[6], J. N. Matthews[3], R. Mayta[6], I. Myers[3], S. Nagataki[10], K. Nakai[6], R. Nakamura[15], T. Nakamura[25], A. Nakazawa[15], E. Nishio[20], T. Nonaka[8], S. Ogio[8], M. Ohnishi[8], H. Ohoka[8], Y. Oku[20], T. Okuda[26], Y. Omura[6], M. Ono[10], A. Oshima[27], S. Ozawa[28], I. H. Park[16], M. Potts[3,29], M. S. Pshirkov[18,30], D. C. Rodriguez[3], C. Rott[3,16], G. I. Rubtsov[18], D. Ryu[31], H. Sagawa[8], N. Sakaki[8], T. Sako[8], N. Sakurai[6], K. Sato[6], T. Seki[15], K. Sekino[8], P. D. Shah[3], Y. Shibasaki[15], N. Shibata[20], T. Shibata[8], J. Shikita[6], H. Shimodaira[8], B. K. Shin[31], H. S. Shin[8], D. Shinto[20], J. D. Smith[3], P. Sokolsky[3], B. T. Stokes[3], T. A. Stroman[3], K. Takahashi[8], M. Takamura[32], M. Takeda[8], R. Takeishi[8], A. Taketa[33], M. Takita[8], Y. Tameda[20], K. Tanaka[34], M. Tanaka[35], S. B. Thomas[3], G. B. Thomson[3], P. Tinyakov[18,22], I. Tkachev[18], H. Tokuno[36], T. Tomida[15], S. Troitsky[18], R. Tsuda[6], Y. Tsunesada[6,9], S. Udo[12], T. Uehama[15], F. Urban[37], D. Warren[10], T. Wong[3], M. Yamamoto[15], K. Yamazaki[27], K. Yashiro[32], F. Yoshida[20], Y. Zhezher[8,18], and Z. Zundel[3]

[1]Department of Physics, Loyola University Chicago, Chicago, IL, USA, [2]National Institute for Space Research (INPE), Sao Jose dos Campos, Brazil, [3]Department of Physics and Astronomy, High Energy Astrophysics Institute, University of Utah, Salt Lake City, UT, USA, [4]Langmuir Laboratory for Atmospheric Research, New Mexico Institute of Mining and Technology, Socorro, NM, USA, [5]Now at NASA Marshall Space Flight Center, Huntsville, AL, USA, [6]Graduate School of Science, Osaka Metropolitan University, Osaka, Japan, [7]Department of Physics, Research Institute of Natural Science, Hanyang University, Seoul, Korea, [8]Institute for Cosmic Ray Research, University of Tokyo, Kashiwa, Japan, [9]Nambu Yoichiro Institute of Theoretical and Experimental Physics, Osaka Metropolitan University, Osaka, Japan, [10]Astrophysical Big Bang Laboratory, RIKEN, Wako, Japan, [11]Now at Department of Astronomy and Astrophysics, University of California, Santa Cruz, CA, USA, [12]Faculty of Engineering, Kanagawa University, Yokohama, Japan, [13]Interdisciplinary Graduate School of Medicine and Engineering, University of Yamanashi, Kofu, Japan, [14]The Graduate School of Science and Engineering, Saitama University, Saitama, Japan, [15]Academic Assembly School of Science and Technology Institute of Engineering, Shinshu University, Nagano, Japan, [16]Department of Physics, SungKyunKwan University, Suwon, South Korea, [17]Department of Physics, Tokyo City University, Tokyo, Japan, [18]Institute for Nuclear Research of the Russian Academy of Sciences, Moscow, Russia, [19]Faculty of Systems Engineering and Science, Shibaura Institute of Technology, Tokyo, Japan, [20]Department of Engineering Science, Faculty of Engineering, Osaka Electro-Communication University, Osaka, Japan, [21]Now at Argonne National Laboratory, Physics Division, Lamont, IL, USA, [22]Service de Physique Théorique, Université Libre de Bruxelles, Brussels, Belgium, [23]Department of Physics, Yonsei University, Seoul, South Korea, [24]Center for Astrophysics and Cosmology, University of Nova Gorica, Nova Gorica, Slovenia, [25]Faculty of Science, Kochi University, Kochi, Japan, [26]Department of Physical Sciences, Ritsumeikan University, Kusatsu, Japan, [27]College of Engineering, Chubu University, Kasugai, Japan, [28]Quantum ICT Advanced Development Center, National Institute for Information and Communications Technology, Tokyo, Japan, [29]Now at Physics Department, Georgia Institute of Technology, Atlanta, GA, USA, [30]Sternberg Astronomical Institute, Moscow M.V. Lomonosov State University, Moscow, Russia, [31]Department of Physics, School of Natural Sciences, Ulsan National Institute of Science and Technology, Ulsan, Korea, [32]Department of Physics, Tokyo University of Science, Noda, Japan, [33]Earthquake Research Institute, University of Tokyo, Tokyo, Japan, [34]Graduate School of Information Sciences, Hiroshima City University, Hiroshima, Japan, [35]Institute of Particle and Nuclear Studies, KEK, Ibaraki, Japan, [36]Graduate School of Science and Engineering, Tokyo Institute of Technology, Tokyo, Japan, [37]CEICO, Institute of Physics, Czech Academy of Sciences, Prague, Czech Republic

Abstract In this paper, we present the first high-speed video observation of a cloud-to-ground lightning flash and its associated downward-directed Terrestrial Gamma-ray Flash (TGF). The optical emission of the event was observed by a high-speed video camera running at 40,000 frames per second in conjunction with the Telescope Array Surface Detector, Lightning Mapping Array, interferometer, electric-field fast antenna, and the National Lightning Detection Network. The cloud-to-ground flash associated with the observed TGF was formed by a fast downward leader followed by a very intense return stroke peak current of −154 kA. The TGF occurred while the downward leader was below cloud base, and even when it was halfway in its propagation to ground. The suite of gamma-ray and lightning instruments, timing resolution, and source proximity offer us detailed information and therefore a unique look at the TGF phenomena.

Plain Language Summary This study provides the very first simultaneous observations of a downward-directed terrestrial gamma-ray flash (TGF) together with its associated cloud-to-ground lightning flash using a high-speed camera in addition to gamma-ray and radio measurements. The camera, running at 40,000 frames per second, allowed us to check the characteristics of the downward leader, the development stage of the lightning flash, and the luminosity variations in coincidence with TGF production.

1. Introduction

Terrestrial Gamma-ray Flashes (TGFs) are bursts of gamma-ray radiation produced via bremsstrahlung in the Earth's atmosphere. TGFs were first observed by the Burst and Transient Source Experiment on the Compton Gamma-Ray Observatory satellite (Fishman et al., 1994; Kouveliotou, 1994). The leading mechanism that produces TGFs is believed to be the Relativistic Runaway Electron Avalanche (RREA) (Gurevich, 1961; Gurevich et al., 1992). The two main theories were developed to interpret the high-fluence TGF observations are the Relativistic Feedback Discharge mechanism (RFD) (Dwyer, 2003, 2012; Dwyer et al., 2013) and the lightning leader models also called the thermal runaway mechanism (Celestin & Pasko, 2011).

In order to understand the physics behind the initiation and propagation of TGFs, satellite experiments (e.g., RHESSI (Gjesteland et al., 2012; Grefenstette et al., 2009; Smith et al., 2005), Fermi (Briggs et al., 2010), AGILE (Marisaldi et al., 2010), Atmosphere-Space Interactions Monitor (ASIM) (Bjørge-Engeland et al., 2022; Heumesser et al., 2021; Lindanger et al., 2022; Neubert et al., 2019)) have detected thousands of TGFs, and more recently several downward-directed TGFs have also been observed from the ground (Abbasi et al., 2018; Belz et al., 2020; Enoto et al., 2017; Hare et al., 2016; Pleshinger et al., 2019; Tran et al., 2015). Despite several TGF observations being reported in the literature, the mechanism responsible for producing them, and how IC/CG discharges relate to TGFs is still not fully understood.

The sequence of the optical observations of lightning flashes in association with TGFs and in conjunction with high/low radio frequency emissions can improve our understanding of the development stage of the lightning discharge when TGFs occur. It could also enhance our understanding of TGF initiation. The RFD mechanism, introduced by Dwyer (2003) and Dwyer et al. (2013), suggests that photons and positrons produce feedback that exponentially increases the number of runaway electrons. If TGFs are byproducts of *relativistic feedback discharges*, they will consist of high-current electric discharges that generate radio emissions similar to lightning. This will produce light in the UV lines. Dwyer et al. (2013) referred to the RFD process as "dark lightning." The thermal runaway electron's production mechanism, on the other hand, assumes very localized regions in space (streamer heads) of a high electric field (10 times larger than the conventional breakdown field) (Dwyer & Uman, 2014). If TGFs are produced through *thermal runaway electrons* in streamers, then this discharge should produce an optical signal before or simultaneously with the production of gamma-ray emission (Xu et al., 2015). These scenarios together with the emission sequence are still under investigation (Alnussirat et al., 2019).

Recent observations from the ASIM (Bjørge-Engeland et al., 2022; Heumesser et al., 2021; Lindanger et al., 2022; Neubert et al., 2019) have revealed, for the first time and, with high timing accuracy, the optical emission timing and strength associated with lightning discharges in coincidence with TGF and Transient Luminous Event observations. The Modular Multi-spectral Imaging Array (Chanrion et al., 2019) on-board ASIM (Neubert et al., 2019), is made of two cameras and high-speed photometers at 337 and 777.4 nm (both used for detecting lightning) with a 100 kHz sampling rate (Ostgaard et al., 2019; Skeie et al., 2022).

This work presents the first simultaneous detection of a downward TGF together with the observation of the associated cloud-to-ground lightning flash by a high-speed camera. The camera, operating at 40,000 images per second, allowed us to examine the development stage of the lightning flash during the occurrence of a TGF. The advantage of proximity to the source and the use of a suite of lightning instruments together with the high-speed camera made possible some further understanding of the characteristics of lightning processes associated with TGF production. It also allowed us to compare the optical emission observations of lightning discharges associated with downward versus upward-moving TGFs.

2. Instrumentation

The observations of downward TGFs, reported in this work, were detected by the Telescope Array Surface Detector (TASD) located in the southwestern desert of Utah. The flashes that produced the TGFs were recorded simultaneously by a high-speed video camera, a Lightning Mapping Array (LMA), a broadband very high frequency (VHF) interferometer, and Fast Antenna (FA). Figure S1 in Supporting Information S1 shows the layout of all of the involved detectors. Each of these detectors is described in detail in Abu-Zayyad et al. (2012), Abbasi et al. (2017, 2018); Belz et al. (2020), and Saba et al. (2022). In this section, we will introduce each of these instruments briefly.

The Telescope Array Surface Detector (TASD) is a ground-based surface detector (SD) primarily designed to observe Ultra High Energy Cosmic Rays (UHECR). With an area coverage of 700 km^2 the TASD is the largest UHECR detector in the Northern Hemisphere. It comprises 507 SDs installed at 1.4 km mean sea level. Each SD unit consists of upper and lower scintillator planes. Each plane is 3 m^2 in area and 1.2 cm in thickness, separated by a 1 mm thick stainless steel sheet. Each plane is read out by individual photomultiplier tubes via wavelengths shifting fiber. The output signals from the photomultipliers are digitized at a 50 MHz sampling rate. Each SD is housed inside an RF-sealed and light-tight stainless-steel enclosure. An event trigger occurs when three adjacent SDs observe a signal greater than 3 Minimum Ionizing Particles within 8 μs (~150 FADC counts). When an event trigger occurs, the signals from all individually triggered SDs within ±32 μs are recorded (Abbasi et al., 2018; Abu-Zayyad et al., 2012). The TASD detector observed approximately 25 downward terrestrial gamma-ray flashes within the past 13 years, making it the world-leading detector in downward TGF observations. Details of the detector's design, trigger, and particle energy can be found in Abu-Zayyad et al. (2012), Abbasi et al. (2018), and Belz et al. (2020).

The High-speed video camera is a monochrome Phantom V2012 operating at 40,000 frames per second with a time interval between frames of 25.00 μs and an exposure time of 23.84 μs (at the end of each frame the camera is blind for 1.14 μs due to data transfer). Each frame of the video is time-stamped by utilizing a GPS antenna and has a resolution of 1,280 × 448 pixels. The camera is sensitive to the visible and near-infrared spectra (400–1,000 nm). The camera was installed 5 km to the east border of the TASD inside a building adjacent to the interferometer (INTF) and the electric-field fast antenna (FA). The 20-mm focal length lens allowed a vertical viewing angle of 35°, and a horizontal angle of 84° covering almost all of the TASD detectors. The camera's position and settings were optimized to observe downward TGF sources that are approximately 30 km from the camera and up to 3 km above ground level. Each video had a recording length of 1.1 s and was automatically triggered by changes in luminosity. Data from the camera is stored on a computer at the site and analyzed offline. The elevation angles from the camera were used to calculate the source height of the TGF sources.

The Lightning Mapping Array (LMA), developed by the Langmuir Laboratory group at New Mexico Tech (Rison et al., 1999; Thomas et al., 2004), has been running at the TASD detector since 2013. The LMA detects the lightning sources emitting impulsive signals between 60 and −66 MHz. LMA-detected sources are analyzed using the time-of-arrival technique of the impulse signal time for multiple triggered LMA stations on the ground. This technique provides us with detailed 3D images of peak VHF radiation events above threshold in 80 μs time intervals. The LMA detects VHF peak with a time accuracy of 35-ns root mean square over a wide (>70 dB) dynamic range, from less than 10 mW to greater than 100 kW peak source power (Thomas et al., 2004).

The INTerFerometer (INTF) and the Fast electric field change Antenna (FA) at the TASD site have been running since 2018. The INTF records broadband (20–80 MHz) waveforms at 180 MHz from three flat-plate receiving antennas. The three antennas were positioned in a triangular baseline of 106–121 m. Such a baseline was used to maximize the angular resolution over the TASD detector. The INTF is processed offline to determine the two-dimensional azimuth and elevation arrival directions of the VHF radiation with sub-microsecond resolution (Stock et al., 2014). The FA, on the other hand, records the electric field changes of lightning discharges. The

FA provides high-resolution 180 MHz measurements of the LF/ELF discharge sferics (Belz et al., 2020; Liu et al., 2019). The FA uses a downward-looking flat plate sensor. The FA data is stored locally and processed offline similar to the INTF data.

3. Observations and Analysis

After the installation of the high-speed video camera on 12 August 2021, we recorded several lightning flashes over the TASD before detecting the first optical observation of lightning discharges associated with downward-directed TGF events on 11 September 2021. On that day nine flashes occurred over the TASD detector. They were all cloud-to-ground flashes with negative polarity. Six of these nine flashes produced TGFs, all of them occurring during a time interval of only 51 min. The three non-producing TGF flashes had return stroke peak currents of less than 26 kA as reported by the National Lightning Detection Network (NLDN). The six gamma-ray initiating flashes, on the other hand, were produced by flashes with peak currents of 51, 67, 53, 154, 134, and 223 kA consecutively as reported by the NLDN. In all the TGF-producing flashes, the TGFs were associated with the downward leader propagation before the first return stroke. Four of the TGF-producing flashes had multiple return strokes. All subsequent strokes had different ground contact points and the first return stroke was the most intense one.

While the TASD has observed about 27 TGFs between 2008 and 2020, this weakly convective, hail-producing storm, has been found to be an uncommon observation of a storm by the TASD. At first, all the TGFs observed on that day were produced by cloud-to-ground flashes with return stroke peak currents that ranged in magnitude from 51 kA all the way to 223 kA. In addition, the maximum energy deposit on one of the SDs had reached energies of up to 33,913 Vertical Equivalent Muons (VEM) (74 GeV). Also, the duration of the observed TGF bursts reached up to 719 μs. Note that previously detected TGFs by the TASD detector typically were produced by flashes with an average peak current of 52 kA and maximum peak current of 139 kA, a deposited maximum energy on a single SD of no more than 997 VEM (2 GeV) and a duration of less than 551 μs.

Most importantly, while the average rate of TGF observations by the TASD detector is about two events per year, this storm resulted in six TGF observations within 1 hr (22% of all TGF observed in the past 13 years). This makes it the highest rate of TGF observations in both one thunderstorm and in all thunderstorm seasons observed by the TASD detector in the southwestern desert of Utah.

In this work, we focus on and make a detailed analysis of the fourth flash during which a TGF is observed at 17:11:12 UTC by the TASD, the high-speed video camera, INTF, and FA. In the following, we refer to this flash as TGF-4. A more detailed analysis of this special storm, and the other five TGF-producing flashes, is now underway and will be reported on in a future publication. We chose the TGF-4 event because it was the clearest and the most straightforward to analyze. This TGF resulted in a bursts of three gamma-ray triggers reported by the TASD detector. We will refer to these triggers as trigger A, B, and C. The gamma-ray footprint and LMA source locations for this TGF are shown in Figures S2 and S3 of the Supporting Information S1. As shown in Figure S2 of the Supporting Information S1, the maximum size of the TGF footprint on the ground, as observed by the TASD, is approximately 6 km in diameter. The maximum energy deposited in a TASD detector was 1.8 GeV. The TGF burst, which occurred during the propagation of a fast leader, lasted for 719 microseconds and was followed by a high peak current return stroke of −154 kA as reported by the NLDN.

The TGF-4-burst A, B, and C trigger sources were produced over the eastward part of the TASD detector with a 10.9 km distance from the high-speed video camera, INTF, and FA location. Trigger A, B, and C source heights were obtained using two independent analyses and were found to be consistent within uncertainties. In the first method, the heights were found using the camera pointing direction and the distance given by the LMA, resulting in heights of 2.5, 1.9, and 1.3 km above ground level for triggers A, B, and C respectively. In the second method, the heights were found using the INTF elevation and azimuthal direction and the distance given by the LMA, utilizing the iteration procedure used in Belz et al., 2020, resulting in heights of 2.4, 1.9, and 1.6 km above ground level. Moreover, the propagational two-dimensional speeds of the leader at triggers A, B, and C were found to be 7.2×10^6 m/s, 2.5×10^6 m/s, and 3.0×10^6 m/s. The speed values reported above are higher than the average stepped leader speeds (Campos et al., 2014). It is also found to be higher than average upward development speeds of intra-cloud discharges during the production of TGFs (Cummer et al., 2015; Shao et al., 2010). Figure 1 shows the lightning flash and the height, elevation, and azimuth of the trigger A, B, and C sources as observed by the high-speed video camera, the INTF, and the TASD detectors.
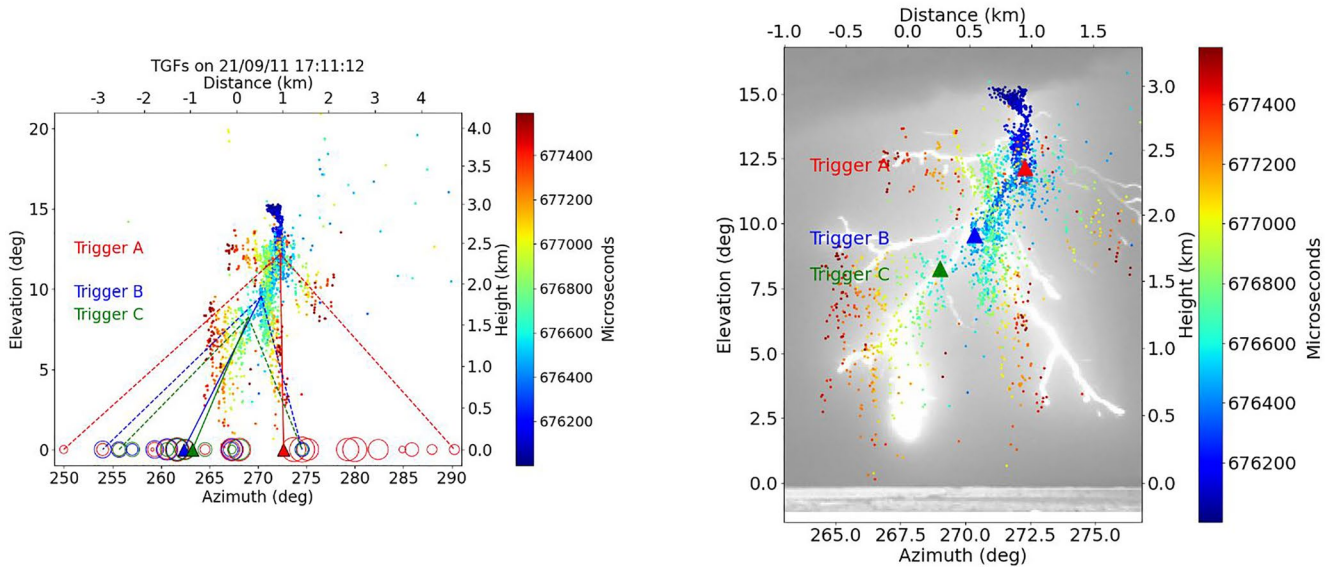
Figure 1. The left-hand plot shows the elevation versus azimuth plots of the INTF observations. The color represents the timing (blue is earlier and red is later in the flash). The red, green, and blue dashed lines point from the source of the TGF for trigger A, B, C and consecutively to the TASD detectors at the edges of the footprint observation on the ground. The circles on the ground refer to the TASD detectors triggered by the TGF observation. The filled circles show the central position of the footprint weighted by the energy deposited in the TASD. The color corresponds to each trigger using the same color code as the dashed lines. The size and color of each circle are proportional to the energy deposited in the scintillator detector logarithmically. The right-hand plot shows the elevation versus azimuth for the whole flash in a frame of the camera in addition to the INTF point sources using the same color scale as the left-hand plot. The filled triangles indicate to the source height for each trigger obtained from the iteration procedure.

The fluence of this flash, determined using a GEANT4 simulation, was estimated to be 3×10^{15}. The GEANT4 simulation used in this work is described in detail in Abbasi et al. (2018), where electrons above 100 keV are generated from a point-like source, according to a RREA spectrum, propagated through the atmosphere, and the TASD detector. Based on our observation of the shower footprint, source position, and leader altitudes, particles are assumed to be forward beamed within a cone of half-angle of 20°.

The optical emission, in this work, was analyzed using the high-speed video camera. Figure 2 shows the progression of the leader of this flash in multiple selected frames as observed by the high-speed video camera. Some of the selected frames display a light saturation problem. This problem is due to the fact the camera's settings were conservatively optimized for suspected multiple scenarios including a very faint signal if the sources of the TGFs
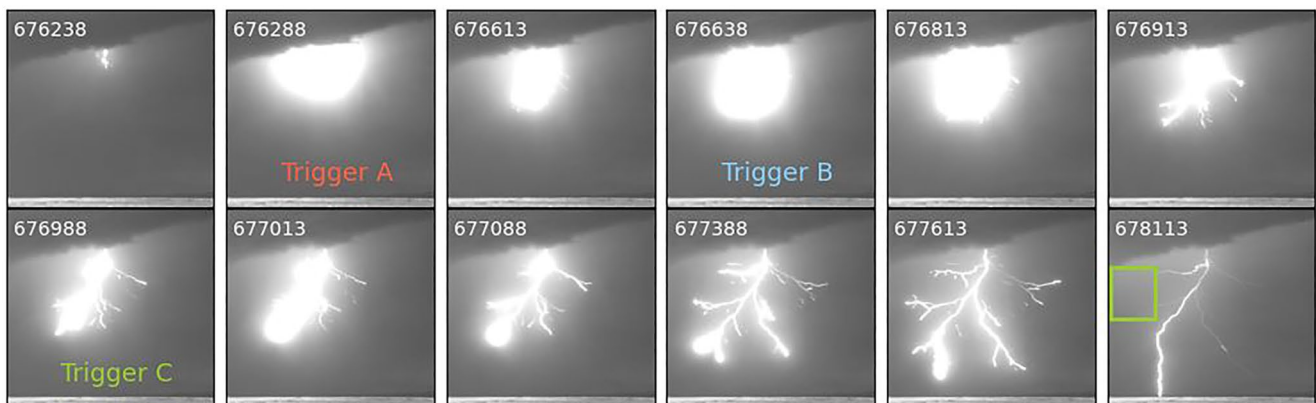
Figure 2. High-speed video selected frames of the TGF producing flash from the time it breaks below the cloud until the return stroke. Note that the time difference between these images does not correspond to the time resolution of the camera. These images are 12 images selected to cover the view of the whole flash (more images from the camera are shown in Figure S5 of the Supporting Information S1). The green square over the last image indicates the area monitored to extract the luminosity variation. The timing in microseconds from 17:11:12 UTC is displayed at the left corner of each image.
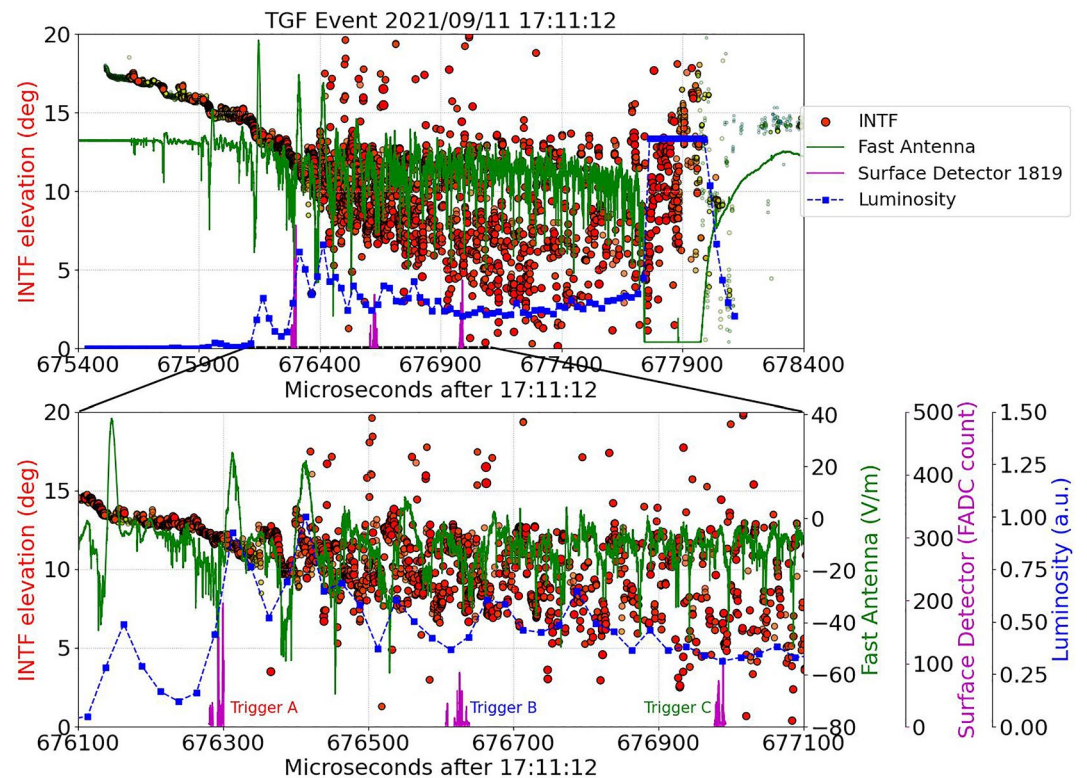
Figure 3. This figure shows the TASD waveforms for one of the Surface Detectors (1,819) in magenta, the average luminosity in dark blue, the electric-field waveform in green, the INTF elevation in red circles (size and color are proportional to the power of the radio signal). Top: The flash observed from initiation until the first return stroke within 3 ms duration. Bottom: a zoomed in version of the top plot within 1 ms.

were inside the cloud and would suffer from light scattering. The initial camera settings would have, in principle, allowed us to detect possible faint signals due to scattering or absorption for up to 30 km away. However, this TGF storm was the most energetic TGF-producing thunderstorm we have ever observed. The fact that the TGF signals were associated with a well-developed, very intense leader which was below the cloud base contributed to the high luminosity. The intense luminosity, high leader speed, and large return-stroke current suggest that the leader had a very high charge density. In two cases (trigger B and C) the leader was almost halfway to the ground at the time of the gamma-ray emissions, as shown in Figure 1.

Figure 3 combines the TASD, high-speed video camera luminosity, INTF, and FA observations. The TGF timing relative to the INTF, electric field change pulses, and visible light emission was calculated using the time matching analysis between the TASD, the INTF, and the LMA as carefully described in detail in Belz et al. (2020). Two different zooms of this flash are displayed. The top panel of Figure 3 shows 3 milliseconds of the detectors' observations, while the bottom panel shows a 1-millisecond zoom. The TASD, INTF, and FA data displayed in this plot are both triggered and analyzed similarly to previous TGFs we reported on in Belz et al. (2020). Note that the first electric field breakdown pulse (at 675,754 µs in Figure 3-top) occurs well before (515 µs) the first TGF burst (at 676,269 µs). The first breakdown pulse, according to the INTF, appears to occur at an approximate height of 3,400 m. However, at the time of the first TGF burst, the leader tip is already well below the cloud base (second frame in Figure 2).

The luminosity, shown in dark blue, is measured by averaging the pixel values of an area adjacent to the lightning flash channel (diffused, not direct luminosity) in each video image. This area is indicated by a green rectangle shown in the last frame presented in Figure 2. The motivation behind this method is to avoid misleading peaks in the luminosity (possible plateaus) that could have been encountered due to the saturation of pixels in several snapshots in Figure 2. Note that we did compare both the average luminosity, including the adjacent pixels to the flash versus the pixels including the flash itself, and found that both intensity curves are consistent with each other (shown in Figure S4 of the Supporting Information S1).

4. Discussion

This work presents the first simultaneous detection of a downward TGF together with the observation of the associated cloud-to-ground lightning flash by a high-speed video camera. The camera allowed us to check the development stage and the luminosity of the lightning leader during the occurrence of an extremely energetic downward-direct terrestrial gamma-ray flash. The detected TGF presented unique features in terms of energy deposit, and duration, and was associated with an unusually fast stepped leader that produced a very high peak current return stroke. Unlike most of the other TASD observed events (Abbasi et al., 2018; Belz et al., 2020), this extremely energetic downward-direct terrestrial gamma-ray is not solely related to the early leader stage. The energetic observed gamma-ray triggers were produced as the leader clearly propagated below the cloud base. The third TGF burst happened when the stepped leader was approximately halfway to the ground. Observing a TGF during the stepping leader further unlocks the circumstances under which TGFs are produced. Such observation may shed light on the lightning-stepping process itself.

X-rays have also been detected during the propagation of energetic stepped and dart leaders to ground in past studies (e.g., Howard et al., 2010; Moore et al., 2001; Saba et al., 2019; Urbani et al., 2021). The typical downward-directed TGF observations by the TASD are from the initial leader stage of lightning flashes 3–5 km above ground level. Other experimental works have also reported TGF observations following return strokes of CG discharges (Dwyer et al., 2012; Ringuette et al., 2013; Tran et al., 2015). X-rays, on the other hand, appeared to be detected during the propagation of energetic stepped and dart leaders a few hundred meters above the ground. X-rays have been observed to have a softer energy spectrum than gamma-rays which are not more than 250 keV (Dwyer et al., 2004). TGFs and X-rays are the two most common energetic radiation during a lightning process. Until now, it is not clear whether TGFs and X-ray emissions detected at ground level are related. That being said, it is important to reiterate, and as discussed in detail in our previous publications (Abbasi et al., 2018; Belz et al., 2020), that the TASD detects multi-MeV gamma-radiation and is blind to X-radiation.

The measured luminosity of the optical emissions observed by the high-speed video camera were found to start to increase within 25 microseconds from the onset of the TGF trigger signal and peak some 25–75 microseconds after the TGF trigger ceases. This may be coincidental, or it could be part of a pattern. We intend to study this further by examining the other TGF observations we made and continue to make at the TASD site, and will report on our findings in future publications. It is interesting to note that Belz et al. (2020) showed that TGF triggers were associated with an electric field pulse (initial breakdown pulse) which was not necessarily the largest one, and that, not all initial breakdown pulses were associated with TGF triggers. Similarly, in Figure 3, we observed that some luminosity peaks occurred after the TGF bursts. They were not necessarily the largest ones and not all the luminosity peaks were associated with TGF triggers.

ASIM collaboration reported on TGF detections with associated optical pulses (Ostgaard et al., 2019; Skeie et al., 2022). They found that the majority are observed to start after a weak increase in the optical emission in the 337 and 777.4 nm photometers, and before, or at the onset of, the main ~2 ms long optical pulse (Ostgaard et al., 2019). In our data, we observe the first TGF trigger roughly 200 µs after the onset of the main optical pulse, as can be seen in Figure 3. However, we note that the TGF occurs near the start of the main optical pulse, which lasts for about 2 ms, and that the optical luminosity increases and peaks after the first TGF trigger. Future analysis of the distribution of the relative time difference between TGFs and the main optical pulses, observations of the UV emissions, and simulation work are planned to better understand this issue.

5. Summary and Future Outlook

On 11 of September 2021, we observed the highest TGF-rate-producing thunderstorm by the TASD. This storm was responsible for a significant fraction of all ground TGFs detected over the TASD in the past 10 years. This work presents the first simultaneous detection of one of those downward-directed TGFs together with the observation of the associated cloud-to-ground lightning flash by a high-speed camera, an INTF, and a FA. In this paper, we investigate the optical emission of a lightning flash associated with an energetic downward TGF. The TASD in addition to the suit of lightning instruments including a high-speed video camera allowed us to understand in detail the height, speed, footprint, energy deposit, and stage of lightning in the flash that is associated with gamma-ray bursts observed by the TASD detector.

Based on the simultaneous use of the TASD, lightning instruments with a high-speed camera recording 40,000 images per second, we observed that:

1. The energetic detected TGF burst occurred during the propagation of a fast and bright downward negative leader which resulted in a high peak current return stroke of −154 kA.
2. The leader was propagating below the cloud base during the TGF burst. The last trigger occurred when it was almost halfway to the ground.
3. The TGF presented unique features in terms of energy deposit and duration.
4. The TGF was produced in an uncommon storm at the TASD site. This single storm was responsible for the detection of a significant fraction of all ground TGFs detected over 10 years.

To understand the physics behind the initiation and propagation of TGFs, and to further compare the optical signature correlation between downward and upward-directed TGF emissions (Bjorge-Engeland et al., 2022; Heumesser et al., 2021; Lindanger et al., 2022; Ostgaard et al., 2019) we have installed photometers at the TASD site. These photometers share the same field of view as the high-speed video camera and will report, with much higher timing resolution, about the optical emissions from atmospheric electrical discharge processes in three different wavelengths: at 337.0 nm (associated with the second positive system of the nitrogen molecule ($2PN_2$)), 391.2 nm (associated with $1NN2^+$ emission correspond to the first negative system of the nitrogen molecule $N2^+$), and 777.4 nm (associated with the atomic oxygen (OI)). This will hopefully allow us to build further conclusions that support the model responsible for the TGF initiation and verify if downward-directed TGFs are a variant of the same phenomenon that causes upward-directed TGFs.

Data Availability Statement

The data used in this paper are available through this link: http://doi.org/10.17605/OSF.IO/WH4UP. They are uploaded in the following directories: The Fast Antenna (FA), the INTerFerometer (INTF), the Lightning Mapping Array (LMA), the high-speed video camera (Optical data), and the Telescope Array Surface Detector (TASD). To be able to look at the optical data, a PCC 3.6 Phantom software is needed. The package was uploaded in the same directory.

References

Abbasi, R., Abe, M., Abu-Zayyad, T., Allen, M., Anderson, R., Azuma, R., et al. (2017). The bursts of high energy events observed by the telescope array surface detector. *Physics Letters A*, *381*(32), 2565–2572. https://doi.org/10.1016/j.physleta.2017.06.022

Abbasi, R., Abu-Zayyad, T., Allen, M., Barcikowski, E., Belz, J., Bergman, D., et al. (2018). Gamma ray showers observed at ground level in coincidence with downward lightning leaders. *Journal of Geophysical Research: Atmospheres*, *123*(13), 6864–6879. https://doi.org/10.1029/2017jd027931

Abu-Zayyad, T., Aida, R., Allen, M., Anderson, R., Azuma, R., Barcikowski, E., et al. (2012). The surface detector array of the telescope array experiment. *Nuclear Instruments and Methods in Physics Research Section A: Accelerators, Spectrometers, Detectors and Associated Equipment*, *689*, 87–97. https://doi.org/10.1016/j.nima.2012.05.079

Alnussirat, S. T., Christian, H. J., Fishman, G. J., Burchfield, J., & Cherry, M. L. (2019). Simultaneous space-based observations of terrestrial gamma-ray flashes and lightning optical emissions: Investigation of the terrestrial gamma-ray flash production mechanisms. *Physical Review D*, *100*(8), 083018. https://doi.org/10.1103/PhysRevD.100.083018

Belz, J., Krehbiel, P., Remington, J., Stanley, M., Abbasi, R., LeVon, R., et al. (2020). Observations of the origin of downward terrestrial gamma-ray flashes. *Journal of Geophysical Research: Atmospheres*, *125*(23), e2019JD031940. https://doi.org/10.1029/2019JD031940

Bjørge-Engeland, I., Østgaard, N., Mezentsev, A., Skeie, C. A., Sarria, D., Lapierre, J., et al. (2022). Terrestrial gamma-ray flashes with accompanying elves detected by ASIM. *Journal of Geophysical Research: Atmospheres*, *127*(11), e2021JD036368. https://doi.org/10.1029/2021JD036368

Briggs, M. S., Fishman, G. J., Connaughton, V., Bhat, P. N., Paciesas, W. S., Preece, R. D., et al. (2010). First results on terrestrial gamma ray flashes from the fermi gamma-ray burst monitor. *Journal of Geophysical Research*, *115*(A7), A07323. https://doi.org/10.1029/2009ja015242

Campos, L. Z., Saba, M. M., Warner, T. A., Pinto, O., Krider, E. P., & Orville, R. E. (2014). High-speed video observations of natural cloud-to-ground lightning leaders—A statistical analysis. *Atmospheric Research*, *135–136*, 285–305. https://doi.org/10.1016/j.atmosres.2012.12.011

Celestin, S., & Pasko, V. P. (2011). Energy and fluxes of thermal runaway electrons produced by exponential growth of streamers during the stepping of lightning leaders and in transient luminous events. *Journal of Geophysical Research*, *116*(A3), A03315. https://doi.org/10.1029/2010ja016260

Chanrion, O., Neubert, T., Lundgaard Rasmussen, I., Stoltze, C., Tcherniak, D., Jessen, N. C., et al. (2019). The modular multispectral imaging array (MMIA) of the ASIM payload on the international space station. *Space Science Reviews*, *215*(4), 28. https://doi.org/10.1007/s11214-019-0593-y

Cummer, S. A., Lyu, F., Briggs, M. S., Fitzpatrick, G., Roberts, O. J., & Dwyer, J. R. (2015). Lightning leader altitude progression in terrestrial gamma-ray flashes. *Geophysical Research Letters*, *42*(18), 7792–7798. https://doi.org/10.1002/2015gl065228

Dwyer, J. R., Schaal, M. M., Cramer, E., Arabshahi, S., Liu, N., Rassoul, H. K., et al. (2012). Observation of a gamma-ray flash at ground level in association with a cloud-to-ground lightning return stroke. *Journal of Geophysical Research*, *117*, A10303. https://doi.org/10.1029/2012ja017810

Dwyer, J. R. (2003). A fundamental limit on electric fields in air. *Geophysical Research Letters*, *30*(20), 2055. https://doi.org/10.1029/2003gl017781

Dwyer, J. R. (2012). The relativistic feedback discharge model of terrestrial gamma ray flashes. *Journal of Geophysical Research*, *117*(A2), A02308. https://doi.org/10.1029/2011ja017160

Dwyer, J. R., Liu, N., & Rassoul, H. K. (2013). Properties of the thundercloud discharges responsible for terrestrial gamma-ray flashes. *Geophysical Research Letters*, *40*(15), 4067–4073. https://doi.org/10.1002/grl.50742

Dwyer, J. R., Rassoul, H. K., Al-Dayeh, M., Caraway, L., Wright, B., Chrest, A., et al. (2004). Measurements of x-ray emission from rocket-triggered lightning. *Geophysical Research Letters*, *31*(5), L05118. https://doi.org/10.1029/2003gl018770

Dwyer, J. R., & Uman, M. A. (2014). The physics of lightning. *Physics Reports*, *534*(4), 147–241. https://doi.org/10.1016/j.physrep.2013.09.004

Enoto, T., Wada, Y., Furuta, Y., Nakazawa, K., Yuasa, T., Okuda, K., et al. (2017). Photonuclear reactions triggered by lightning discharge. *Nature*, *551*(7681), 481–484. https://doi.org/10.1038/nature24630

Fishman, G. J., Bhat, P. N., Mallozzi, R., Horack, J. M., Koshut, T., Kouveliotou, C., et al. (1994). Discovery of intense gamma-ray flashes of atmospheric origin. *Science*, *264*(5163), 1313–1316. https://doi.org/10.1126/science.264.5163.1313

Gjesteland, T., Østgaard, N., Collier, A. B., Carlson, B. E., Eyles, C., & Smith, D. M. (2012). A new method reveals more TGFs in the RHESSI data. *Geophysical Research Letters*, *39*(5), L05102. https://doi.org/10.1029/2012GL050899

Grefenstette, B. W., Smith, D. M., Hazelton, B. J., & Lopez, L. I. (2009). First RHESSI terrestrial gamma ray flash catalog. *Journal of Geophysical Research*, *114*(A2), A02314. https://doi.org/10.1029/2008JA013721

Gurevich, A. (1961). On the theory of runaway electrons. *Soviet Physics—JETP*, *12*(5), 904–912.

Gurevich, A., Milikh, G., & Roussel-Dupre, R. (1992). Runaway electron mechanism of air breakdown and preconditioning during a thunderstorm. *Physics Letters A*, *165*(5), 463–468. https://doi.org/10.1016/0375-9601(92)90348-P

Hare, B. M., Uman, M. A., Dwyer, J. R., Jordan, D. M., Biggerstaff, M. I., Caicedo, J. A., et al. (2016). Ground-level observation of a terrestrial gamma ray flash initiated by a triggered lightning. *Journal of Geophysical Research: Atmospheres*, *121*(11), 6511–6533. https://doi.org/10.1002/2015jd024426

Heumesser, M., Chanrion, O., Neubert, T., Christian, H. J., Dimitriadou, K., Gordillo-Vazquez, F. J., et al. (2021). Spectral observations of optical emissions associated with terrestrial gamma-ray flashes. *Geophysical Research Letters*, *48*(4), 2020GL090700. https://doi.org/10.1029/2020GL090700

Howard, J., Uman, M. A., Biagi, C., Hill, D., Jerauld, J., Rakov, V. A., et al. (2010). Rf and X-ray source locations during the lightning attachment process. *Journal of Geophysical Research*, *115*(D6), D06204. https://doi.org/10.1029/2009jd012055

Kouveliotou, C. (1994). BATSE results on observational properties of gamma-ray bursts. *The Astrophysical Journal Supplement*, *92*, 637–642. https://doi.org/10.1086/192032

Lindanger, A., Skeie, C. A., Marisaldi, M., Bjørge-Engeland, I., Østgaard, N., Mezentsev, A., et al. (2022). Production of terrestrial gamma-ray flashes during the early stages of lightning flashes. *Journal of Geophysical Research: Atmospheres*, *127*(8), e2021JD036305. https://doi.org/10.1029/2021JD036305

Liu, N., Dwyer, J. R., Tilles, J. N., Stanley, M. A., Krehbiel, P. R., Rison, W., et al. (2019). Understanding the radio spectrum of thunderstorm narrow bipolar events. *Journal of Geophysical Research: Atmospheres*, *124*(17–18), 10134–10153. https://doi.org/10.1029/2019jd030439

Marisaldi, M., Fuschino, F., Labanti, C., Galli, M., Longo, F., Del Monte, E., et al. (2010). Detection of terrestrial gamma ray flashes up to 40 MeV by the AGILE satellite. *Journal of Geophysical Research*, *115*(A3), A00E13. https://doi.org/10.1029/2009ja014502

Moore, C. B., Eack, K. B., Aulich, G. D., & Rison, W. (2001). Energetic radiation associated with lightning stepped-leaders. *Geophysical Research Letters*, *28*(11), 2141–2144. https://doi.org/10.1029/2001GL013140

Neubert, T., Ostgaard, N., Reglero, V., Blanc, E., Chanrion, O., Oxborrow, C., et al. (2019). The ASIM mission on the international space station. *Space Science Reviews*, *215*(2), 26. https://doi.org/10.1007/s11214-019-0592-z

Ostgaard, N., Neubert, T., Reglero, V., Ullaland, K., Yang, S., Genov, G., et al. (2019). First 10 months of TGF observations by ASIM. *Journal of Geophysical Research: Atmospheres*, *124*(24), 14024–14036. https://doi.org/10.1029/2019jd031214

Pleshinger, D. J., Alnussirat, S. T., Arias, J., Bai, S., Banadaki, Y., Cherry, M. L., et al. (2019). Gamma ray flashes produced by lightning observed at ground level by TETRA-II. *Journal of Geophysical Research: Space Physics*, *124*(11), 9229–9238. https://doi.org/10.1029/2019ja026820

Ringuette, R., Case, G. L., Cherry, M. L., Granger, D., Guzik, T. G., Stewart, M., & Wefel, J. P. (2013). Tetra observation of gamma-rays at ground level associated with nearby thunderstorms. *Journal of Geophysical Research: Space Physics*, *118*(12), 7841–7849. https://doi.org/10.1002/2013JA019112

Rison, W., Thomas, R. J., Krehbiel, P. R., Hamlin, T., & Harlin, J. (1999). A GPS-based three-dimensional lightning mapping system: Initial observations in central New Mexico. *Geophysical Research Letters*, *26*(23), 3573–3576. https://doi.org/10.1029/1999gl010856

Saba, M. M. F., da Silva, D. R. R., Pantuso, J. G., & da Silva, C. L. (2022). Close view of the lightning attachment process unveils the streamer zone fine structure. *Geophysical Research Letters*, *49*(24), e2022GL101482. https://doi.org/10.1029/2022GL101482

Saba, M. M. F., Ferro, M. A. S., Cuadros, E. T., Custódio, D. M., Nag, A., Schumann, C., et al. (2019). High-speed video observation of a dart leader producing X-rays. *Journal of Geophysical Research: Space Physics*, *124*(12), 10564–10570. https://doi.org/10.1029/2019ja027247

Shao, X., Hamlin, T., & Smith, D. M. (2010). A closer examination of terrestrial gamma ray flash related lightning processes. *Journal of Geophysical Research*, *115*(A6), A00E30. https://doi.org/10.1029/2009ja014835

Skeie, C. A., Østgaard, N., Mezentsev, A., Bjørge-Engeland, I., Marisaldi, M., Lehtinen, N., et al. (2022). The temporal relationship between terrestrial gamma-ray flashes and associated optical pulses from lightning. *Journal of Geophysical Research: Atmospheres*, *127*(17), e2022JD037128. https://doi.org/10.1029/2022JD037128

Smith, D. M., Lopez, L. I., Lin, R. P., & Barrington-Leigh, C. P. (2005). Terrestrial gamma-ray flashes observed up to 20 MeV. *Science*, *307*(5712), 1085–1088. https://doi.org/10.1126/science.1107466

Stock, M., Akita, M., Krehbiel, P., Rison, W., Edens, H., Kawasaki, Z., & Stanley, M. (2014). Continuous broadband digital interferometry of lightning using a generalized cross-correlation algorithm. *Journal of Geophysical Research: Atmospheres*, *119*(6), 3134–3165. https://doi.org/10.1002/2013jd020217

Thomas, R. J., Krehbiel, P. R., Rison, W., Hunyady, S. J., Winn, W. P., Hamlin, T., & Harlin, J. (2004). Accuracy of the lightning mapping array. *Journal of Geophysical Research*, *109*(D14), D14207. https://doi.org/10.1029/2004jd004549

Tran, M. D., Rakov, V., Mallick, S., Dwyer, J., Nag, A., & Heckman, S. (2015). A terrestrial gamma-ray flash recorded at the Lightning Observatory in Gainesville, Florida. *Journal of Atmospheric and Solar-Terrestrial Physics*, *136*, 86–93. https://doi.org/10.1016/j.jastp.2015.10.010

Urbani, M., Montanyà, J., van der Velde, O. A., López, J. A., Arcanjo, M., Fontanes, P., et al. (2021). High-energy radiation from natural lightning observed in coincidence with a VHF broadband interferometer. *Journal of Geophysical Research: Atmospheres*, *126*(7), e2020JD033745. https://doi.org/10.1029/2020JD033745

Xu, W., Celestin, S., & Pasko, V. P. (2015). Optical emissions associated with terrestrial gamma ray flashes. *Journal of Geophysical Research: Space Physics*, *120*(2), 1355–1370. https://doi.org/10.1002/2014ja020425